

California heat waves: their spatial evolution, variation, and coastal modulation by low clouds

Rachel E. S. Clemesha¹  · Kristen Guirguis¹ · Alexander Gershunov¹ · Ivory J. Small² · Alexander Tardy²

Received: 26 May 2017 / Accepted: 20 August 2017 / Published online: 10 October 2017
© Springer-Verlag GmbH Germany 2017

Abstract We examine the spatial and temporal evolution of heat waves through California and consider one of the key modulating factors of summertime coastal climate—coastal low cloudiness (CLC). Heat waves are defined relative to daytime maximum temperature (T_{\max}) anomalies after removing local seasonality and capture unseasonably warm events during May–September. California is home to several diverse climate regions and characteristics of extreme heat events are also variable throughout these regions. Heat wave events tend to be shorter, but more anomalously intense along the coast. Heat waves typically impact both coastal and inland regions, although there is more propensity towards coastally trapped events. Most heat waves with a strong impact across regions start at the coast, proceed inland, and weaken at the coast before letting up inland. Typically, the beginning of coastal heat waves are associated with a loss of CLC, followed by a strong rebound of CLC starting close to the peak in heat wave intensity. The degree to which an inland heat wave is expressed at the coast is associated with the presence of these low clouds. Inland heat waves that have very little expression at the coast tend to have CLC present and an elevated inversion base height compared with other heat waves.

Keywords Marine layer · Heat waves · Coastal climate · Low clouds

1 Introduction

Heat waves top the list of the deadliest weather extremes in the United States (National Weather Service 2012). In California, heat waves since the 1940s are trending towards more intense, long-lasting, and spatially extensive events (Gershunov et al. 2009). The greatest event on record occurred in July 2006 and resulted in over 600 excess deaths (Ostro et al. 2009), over 1200 excess hospitalizations (Guirguis et al. 2014), and over 16,000 excess emergency-department visits (Knowlton et al. 2009), with disproportionate effects along the coast, even relative to dense coastal population. This event along with 18 other heat waves with significant health impacts were identified by Guirguis et al. (2014) who found that health impacts, measured by unscheduled hospitalizations, in coastal regions were more clear and severe than those for inland regions. These “heat-health events” included many early season heat waves, such as the one in May 2008 for which, after accounting for duration, excess hospitalizations were even more severe than during the July 2006 heat wave. These findings point to the role of local acclimation in vulnerability and health risk. Furthermore, analyses of downscaled Global Climate Model (GCM) projections suggest that heat wave activity is on the rise throughout California, and the greatest intensification is expected to occur along the coast (Gershunov and Guirguis 2012). Indeed, coastal heat wave activity in California has already increased, especially at the North Coast (Gershunov and Guirguis 2012). A focus on coastal heat wave processes is warranted.

Electronic supplementary material The online version of this article (doi:10.1007/s00382-017-3875-7) contains supplementary material, which is available to authorized users.

✉ Rachel E. S. Clemesha
rclemesha@ucsd.edu

¹ Scripps Institution of Oceanography, University of California, San Diego, 9500 Gilman Drive, Mail Code: 0230, La Jolla, CA 92093, USA

² NOAA/National Weather Service, San Diego, CA, USA

Coastal California is exposed to a number of weather and climate influences that are unique to the coastal zone. Among these is the modulating influence of the cool Pacific Ocean, which along with subtropical subsidence, promotes conditions favorable to seasonally persistent, yet variable, coastal low cloudiness (CLC, e.g. Klein and Hartmann 1995). These blanket-like marine stratiform clouds (stratus, stratocumulus, fog, and colloquially marine layer) reduce daytime maximum temperatures (T_{\max}) via their albedo effect (Iacobellis and Cayan 2013). The Southern California Bight is normally cloudiest in June, although the inland extent of the low clouds into coastal Southern California is typically farther in May. The core of maximum seasonal CLC migrates up the coast reaching just north of San Francisco in late July (Clemesha et al. 2016). Daily variability of CLC is positively related most strongly to T_{\max} ~650–800 km to the north rather than directly overhead or inland (Clemesha et al. 2017). Rather than the high temperatures pulling CLC inland in a simple sea breeze intensification, the offset T_{\max} –CLC relationship is partly due to the association between T_{\max} overland and measures of stability, which are linked through large scale atmospheric subsidence patterns. Even though marine layer clouds influence summertime coastal climate, they are not well represented in GCMs. Recently some progress has been made in capturing modes of CLC variability with a coupled regional climate model which suggests slight future CLC declines (O'Brien 2011; O'Brien et al. 2012), which would bolster heat wave activity along the coast. Improved understanding of CLC's role in modulating coastal heat waves is needed in order to better interpret the GCM projected results of coastal heat wave intensification.

Individual case studies have been used to study the interaction between anomalously warm weather and coastal fog formation in the context of large-scale transient systems (Lewis et al. 2003) and to initialize model simulations (Koraćin et al. 2005). Both the mid-April case of Lewis et al. (2003) and the mid-May case of Koraćin et al. (2005), are described in terms of the Leipper (1994) fog formation mechanism. A key component of this mechanism is the inland movement of the North Pacific High and subsequent offshore winds which modify the temperature inversion capping the marine boundary layer (MBL) and the low clouds. This pressure shift also induces strong inland heating that can reach the coast. That is, the synoptic set-up to fog formation described by Leipper (1994) is, as Koraćin et al. (2005) call it, a hot spell. The persistent ridge and offshore warm dry advection of this type of hot spell, lowers the inversion base and enhances longwave radiative cooling at cloud top.

This modulation of the inversion is used by the forecasting community and is described in detail in a NOAA handbook for extreme southwestern California (Small 2006). Computer model resolution has dramatically improved

prediction of inversion characteristics such as inversion base height and strength, thus allowing smaller-scale features related to heat wave expression to be better diagnosed and predicted. Some of these heat wave events are now highly predictable. Conditions with high resolution models showing anomalously high pressure ridging directly overhead with strong east surface winds extending out over the coastal waters create heat waves that fit into this “highly predictable” category. However, for the more marginal cases predictability is still very challenging, (for example, when low level coastal eddy circulations battle successfully against marginal subsidence and offshore flow above the MBL air for anomalously deep MBL and/or stubborn coastal low cloudiness). Such marginal conditions are notorious for occurring at the beginning and end of heat wave events as well. Reliance on observational tools such as satellite imagery, surface pressure gradients, upper air data, and overall pattern recognition (as explored later) is imperative in order to diagnose what the models still cannot properly detect, and ultimately utilize for inversion prediction, especially for short term forecasting.

Large-scale synoptic patterns associated with North American heat waves have been summarized by Grotjahn et al. (2016), while Gershunov and Guirguis (2012) analyzed and described observed and projected heat wave trends for six regions of California. Although observed and projected trends vary by California region, the evolution and communication of heat waves in space and time among coastal and inland regions of California have not been examined in detail. Outstanding questions remain. For example, do specific heat waves manifest differently in different regions; how do they propagate in space? Likewise, under conditions that drive Central Valley heat waves, as described by Grotjahn and Faure (2008), what is occurring at the coast where heat may be modulated or enhanced by the presence or absence of low-level clouds?

In order to address these current gaps, the research objectives of this work are to (1) improve the understanding of heat waves in California and particularly their expressions along the coast as they are modulated by coastal low clouds, (2) describe the spatial and temporal progression of extreme heat events through California, and (3) assess what determines if an inland heat wave will have a strong impact at the coast. We achieve these objectives by investigating (1) heat waves using a high resolution long term gridded data-set of daily temperature, and examining inland and coastal regions of northern and southern California, (2) CLC from coastal airport observations, and (3) large scale synoptic variables from reanalysis.

2 Data and methods

Table 1 and Fig. 1 summarize metrics described in this section and used throughout the paper.

2.1 Data and Heat Wave Index (HWI) definitions

We used a 12 km gridded data-set of daytime maximum temperature (T_{max}) over California for May–September

1949–2010 (Maurer et al. 2002). We define a heat wave index (HWI) in a peaks over threshold (POT) method as exceedances greater than the 95th percentile as in previous studies (e.g. Gershunov et al. 2009; Gershunov and Guirguis 2012). In this work we wish to focus mostly on unseasonable warm events in addition to the more traditionally defined heat waves. Therefore, we apply the POT method to T_{max} anomalies calculated by fitting and removing a double harmonic seasonal cycle over a base period of 1950–2000.

Table 1 Definitions and description of metrics used in this paper

Variable	definition/description
Heat Wave Index (HWI)	Exceedance greater than the 95th percentile of T_{max} anomaly (de-seasonalized raw T_{max})
“Heat wave days”	HWI > 0 °C
“Heat wave event”	Consecutive days with HWI > 0 °C
Peak Magnitude Ratio (PMR)	Peak HWI of paired region : peak HWI of focus region Peak HWI of paired region found during ± 1 day of focus region heat wave event duration. See Fig. 1 schematic PMR < 1, heat wave magnitude greater at focus region PMR > 1, heat wave magnitude greater at paired region PMR = 1, heat wave magnitude same at both regions
Weighted Peak Timing	Hourly time at which half the total event cumulative HWI sum is reached. See Fig. 1 schematic
Raw Heat Wave Index (HWI _{raw})	Exceedance greater than the 95th percentile of raw T_{max} . Definition used for previous work e.g. Gershunov et al. (2009) and Gershunov and Guirguis (2012), but used sparingly in this paper

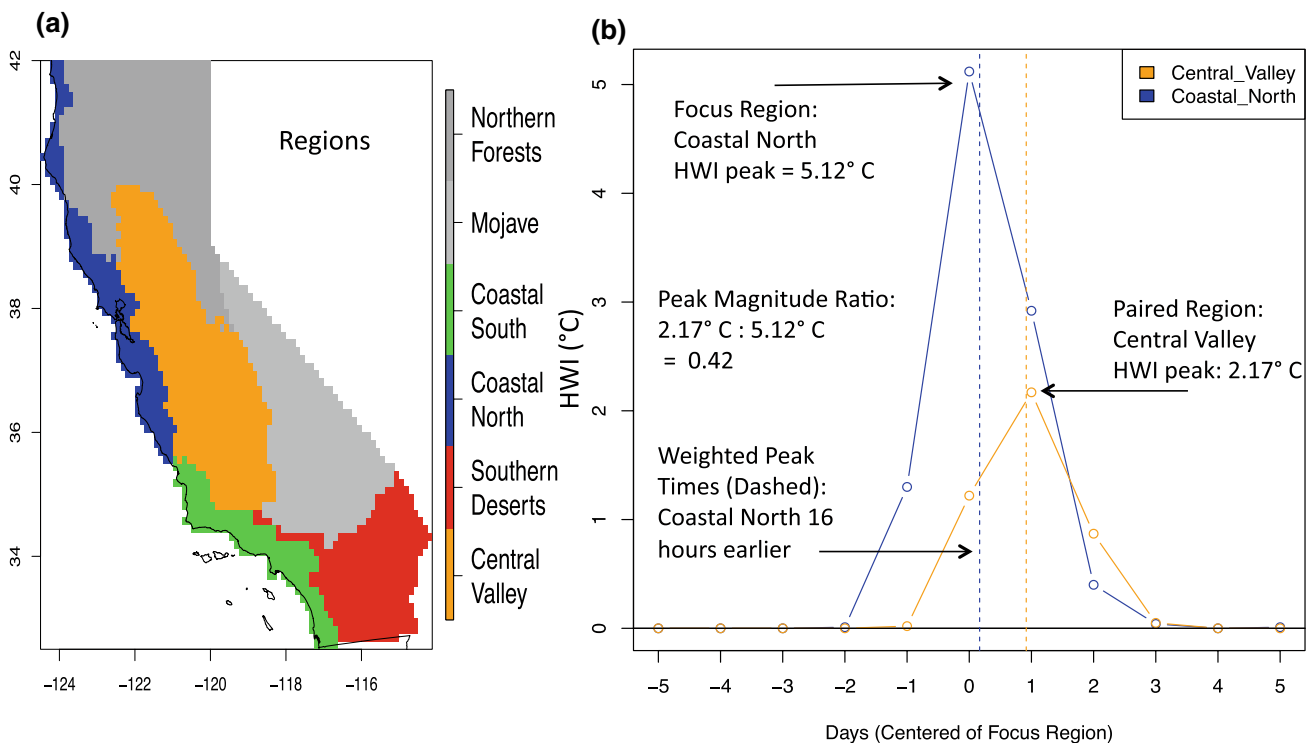


Fig. 1 **a** The six climate regions of California defined empirically by Gershunov and Guirguis (2012), where the *four colored regions* are the focus regions used in this paper. **b** Case study depicting definitions of peak magnitude ratio and weighted peak times. This 2000 case study is the fourth highest ranking Coastal North heat wave.

Since the Coastal North is the focus region, the peak magnitude ratio is calculated here as Central Valley peak HWI: Coastal North peak HWI. *Dashed lines* denote weighted peak times. This was a heat-health event identified by Guirguis et al. 2014

For the purposes of comparison, we also apply the POT method to T_{\max} , which is the more traditional approach. In our discussion, when we apply the POT method to raw, unfiltered T_{\max} , we denote this index as “HWI_raw”, whereas when the POT is applied to T_{\max} anomalies, we denote it as “HWI”. See Fig. 2 for visual display. Heat waves can also be defined relative to nighttime temperatures (Gershunov et al. 2009), but, since the shading and daytime cooling provided by clouds is a primary interest here, we chose to focus on anomalous daytime temperatures.

2.2 Regionalization, heat wave events, ranks, and coastal-inland pairs

We regionalize the gridded HWI using California climate regions defined empirically by Gershunov and Guirguis (2012). Specifically, we calculate the HWI for each California grid cell, and then average the gridded HWI over all grid cells for the South Coast, Southern Deserts, North Coast, and Central Valley regions. We focus on these four regions (out of six) because we wish to track the spatial expression of heat waves affecting the coast. The Coastal North and

Coastal South represent our coastal impact regions of interest, and the Southern Deserts and Central Valley represent our inland regions (Fig. 1a). Note that while at the local grid level a heat wave day (HWI > 0 °C) occurs for 5% of days ($n \sim 474$ days) by definition, the regional heat wave days occur more often and the frequency varies between regions. When examining regional aggregate statistics, the number of heat wave days in each region varies due to the different region sizes and heat wave spatial footprints (heat wave days $n = 3028, 1667, 2574, 1425$, North Coast, Central Valley, South Coast, and Southern Deserts, respectively).

Heat wave events are defined as consecutive days with regional HWI > 0 °C. An event focused approach (rather than e.g. average of HWI over a month), allows for examination of how events propagate in time and space through California. Heat wave events are ranked by the magnitude of the peak day (greatest HWI of event). To focus on the strongest events and to have the same sample size between regions, key analyses use varying thresholds (e.g. top 5 or top 50) of greatest regional heat wave events. Unless otherwise mentioned, analyses are conducted on the top 50 events, in which there are no heat wave events of 1 day duration. To facilitate

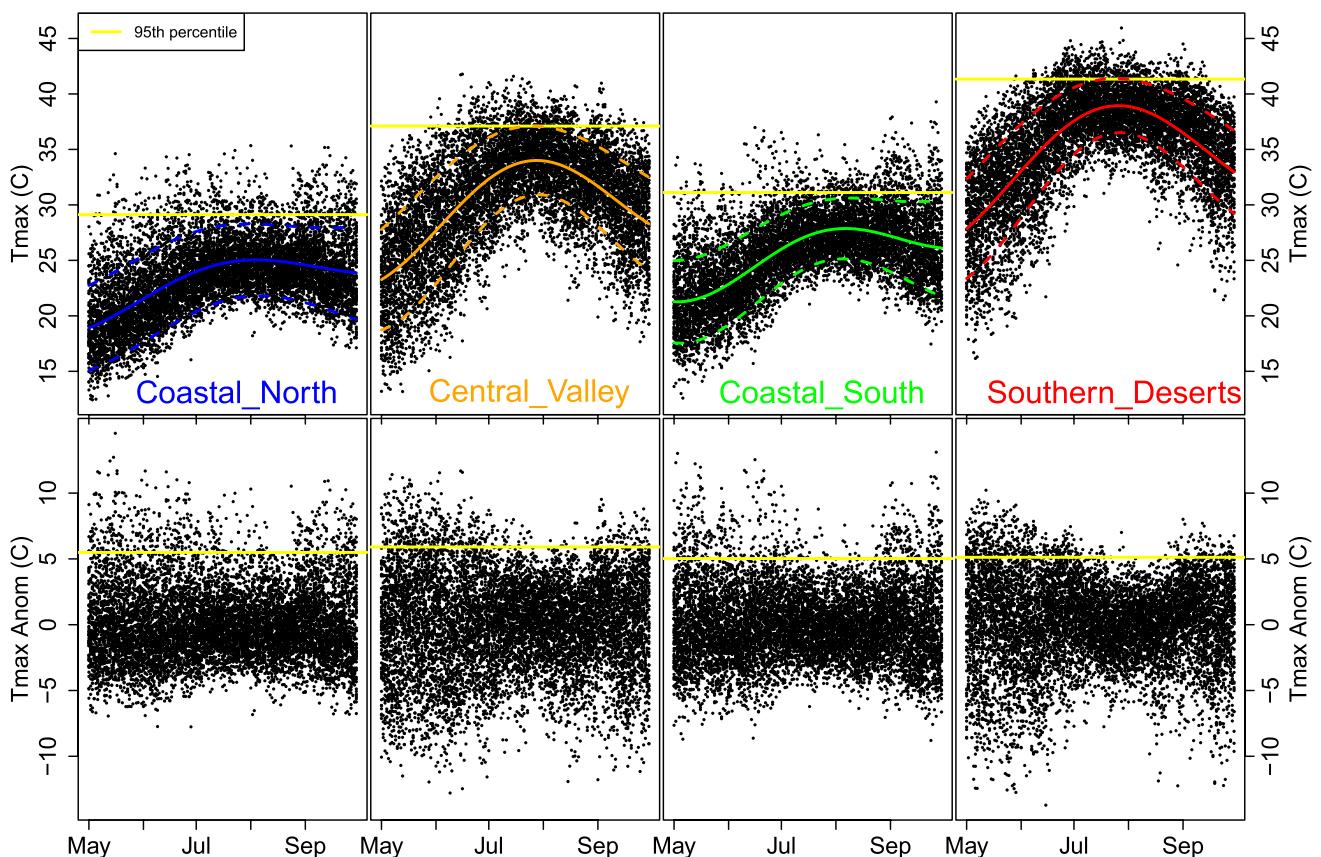


Fig. 2 Regional averaged raw T_{\max} (top) and T_{\max} anomalies (bottom) for 1950–2010. Seasonal Cycle (bold) and ± 1 standard deviation (dashed). 95th percentile (yellow). Days above the 95th percentile of

T_{\max} anomaly (raw T_{\max}) have a HWI > 0 (HWI_raw > 0). Note the regional seasonal cycles shown here are for illustrative purposes. Seasonal cycles are fit and removed to each grid cell

impact-related studies, tables of the peak date and peak HWI of the top 50 heat wave events for each of the four regions are provided in Online Resources 1–4.

To examine the spatial expression and propagation of heat waves, pairs of regions are examined. In particular, we are interested in the relationship between heat waves at the coast and heat waves inland in order to understand the role of CLC. We designate a “focus region” and a “paired region”. The pairs will be denoted as “focus region–paired region”. We examine the coastal inland pairs of “North Coast–Central Valley”, “Central Valley–North Coast”, “South Coast–Southern Deserts”, and “Southern Deserts–South Coast”. Additionally, the findings of Clemesha et al. (2017) motivate the north–south pairing of “Central Valley–South Coast”. Composites are centered on the peak day of a heat event in the focus region, and the spatial expression is examined by comparing the HWI in the focus region with the HWI in the paired region. Ranking selection is done for the focus region, and the magnitude of the heat wave in the paired region is examined. For example, considering an analysis of a South Coast heat wave, if the HWI in the paired region (the Southern Deserts) is near zero, then we can conclude that this heat wave was coastally trapped. However, if the HWI in the paired region is large, then this heat wave was experienced in both regions.

2.3 Spatial and temporal heat wave metrics

To quantify the spatial impact of a heat wave event, we calculated a peak magnitude ratio (PMR). During the duration ± 1 day of a heat wave in the focus region, we calculated the peak HWI magnitude for the focus region (e.g. North Coast in Fig. 1), as well as the paired region (e.g. Central Valley). The PMR is taken as the ratio of peak HWI magnitudes for the paired region to the focus region. In the example shown in Fig. 1b, there is a very strong heat wave in the Coastal North (peak HWI = 5.12 °C). This heat wave is also felt in the Central Valley (peak HWI = 2.17 °C). The peak magnitude ratio (PMR) is 0.42, indicating a much larger impact at the coast than inland (see Table 1 for description). There are some cases when 2 days of equal HWI are identified, and in these cases the day closest to the focus region peak day is used. Note the peak days need not be on the same day in both regions.

To quantify the temporal movement of a heat wave event, we calculated a weighted peak timing. During the duration of a heat wave in the focus region (e.g. North Coast in Fig. 1), the heat wave event at the paired region (e.g. Central Valley) with the most overlapping days is identified. Over each heat wave event duration, we linearly interpolate the daily HWI to an hourly HWI. We cumulatively sum the hourly HWI and identify the time at which half the total event cumulative sum is reached. This time is the weighted

peak time. When the peak magnitude ratio is < 0.20 the heat wave is considered sub-regional. Since sub-regional heat waves do not strongly influence both regions, weighted peak times are not compared. Figure 1 displays the peak magnitude ratio and weighted peak timing definitions for a case study. From Fig. 1b, the weighted peak timing indicates the heat wave peaked 16 h earlier in the Coastal North than in the Central Valley.

2.4 Cloudiness and meteorological data-sets

Low cloud is identified at California coastal airports as in Schwartz et al. (2014), but over all available observations in a 24 h period. Low cloud is defined as cloud with 1 km base height or lower. North coastal low cloudiness (CLC) refers to an average of cloudiness at Arcata (KACV), Oakland (KOAK), San Francisco (KSFO), and Monterey (KMRY). South CLC refers to an average of cloudiness at Los Angeles (KLAX); Long Beach (KLGB); San Diego (KSAN); and North Island (KNZY).

Near-surface winds (sigma level 0.995), vertical velocity at 850 hPa (ω_{850}), sea level pressure (SLP), and geopotential heights at 500 hPa (Z500) were obtained from NCEP/NCAR R-1 (Kalnay et al. 1996). Anomalies were calculated by fitting and removing a double harmonic seasonal cycle over 1948–2014.

We used radiosonde measurements taken at 12 UTC at San Diego (KNKX) and Oakland (KOAK) (available at NOAA/ESRL Radiosonde Database at esrl.noaa.gov/raobs). A temperature inversion is identified when warm air is above cooler air. We calculated inversion base height (ZBASE) and strength (DT) as in Iacobellis et al. (2010). Where ZBASE is the lowest elevation before warming begins, and inversion strength is the difference in temperature between the top and bottom of the inversion.

3 Results and discussion

3.1 Heat waves in a region of diverse climates

The summertime climates of the California coastal regions are substantially cooler than the inland regions (Fig. 2 top). Normal temperatures inland would represent a major heat wave at the coast. For example, the 95th percentile of raw T_{\max} for the North Coast (29.1 °C) is comparable to an average early May or early June day in the Southern Deserts and Central Valley, respectively. In addition to cooler summertime temperatures, the coastal regions also experience a smaller seasonal cycle range relative to the inland regions. Accordingly, when heat waves are defined using the raw T_{\max} 95th percentile threshold (HWI_{raw}), inland heat waves are clustered during the mid-summer seasonal cycle peak.

When the seasonal cycle is removed from each region, and the 95th percentile threshold applied to the resulting T_{max} anomaly, a different pattern of heat wave days emerges (Fig. 2 bottom). This is due to the seasonal variability in T_{max} variance itself. Since there is more variability in the shoulder months, especially early season, more heat waves occur in May compared to the HWI_raw definition. In the inland areas the hottest time of summer also tends to be the least variable, and so there are fewer anomalous hot days in July–August than in the shoulder months.

3.2 May 2008 case study

The highest ranking single heat wave for all 4 regions is in early May 2008. This event ranked 1st, 5th, 18th, and 3rd for North Coast, Central Valley, South Coast, and Southern Deserts, respectively. The peak temperature for each

region was 34.62, 36.25, 32.03, and 40.13 °C, respectively, while the peak HWI for each region was 7.70, 4.64, 4.32, and 3.97 °C above the grid local 95th percentile thresholds. So, although it was hottest in the Southern Deserts, the heat wave magnitude was greatest for the North Coast. The propagation through time and space of this heat wave is shown in Fig. 3. The heat wave starts at the North Coast, spreads inland and south, and then ends first at the coast and last across inland areas. For the North Coast region the event peaks on May 16th; on May 17th the extreme heat has weakened there, but peaks inland in the Central Valley and south at the South Coast. Two days later on May 19th the extreme heat peaks in the Southern Deserts. Below in Sect. 3.5 we investigate if this movement from coast to inland represented here by this extreme case study is observed in a more general sense when we consider larger sample sizes.

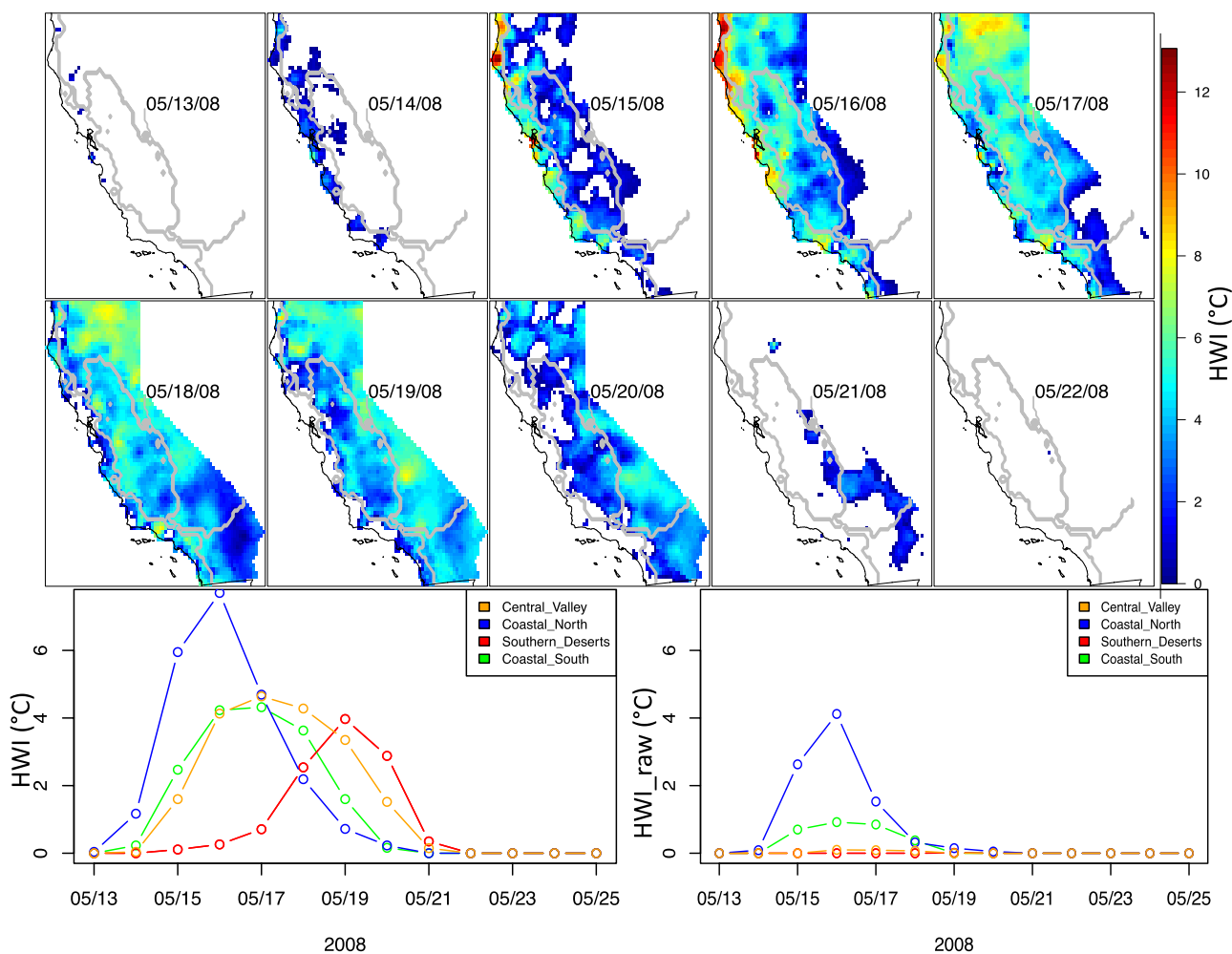


Fig. 3 May 2008 case study. *Top* maps of gridded HWI, for May 13, 2008 to May 22, 2008. *Gray contours* denote region boundaries. *White* signifies HWI=0. *Bottom* time series of regional HWI (*left*),

and HWI_raw (*right*). See Fig. S1 for maps of HWI_raw and CLC time series. Main figures hereinafter use HWI defined on T_{max} anomalies

If the heat wave evolution is viewed in raw T_{\max} sense instead of T_{\max} anomaly [Fig. 3 bottom; maps Figure S1 in online resource], this event appears not as intense for all regions, and particularly for the inland regions where the event barely triggers the threshold. May events for inland areas tend to be unseasonably extreme, but not extreme compared to mid-summer average heat, which is why the event registers as more intense in Fig. 3 using the POT method calculated on T_{\max} anomalies as compared to Figure S1 that uses the POT method calculated on raw T_{\max} . Guirguis et al. (2014) identified this May 2008 event as a heat-health impactful event for the whole state, and regionally for the North Coast and Central Valley. Their heat-health events were conditioned on health data and defined on raw T_{\max} without requiring any threshold exceedance. They show that the health burden of this May event was high. After accounting for duration, the excess hospitalizations during the May 2008 event were even more severe than during the July 2006 heat wave. This event ranks 4th highest in terms of excess hospitalization quantile. Of their 19 heat-health events, 8 (42%) occurred particularly in May. The

health impacts of this May 2008 event, and other heat-health impactful May events in the Central Valley suggest that heat waves defined by anomalies are important and should not be ignored even though these may not be extreme events in a raw T_{\max} sense. Accordingly, since we are interested in describing heat waves with impacts on human health, for the remainder of this paper we will define heat waves based on T_{\max} anomalies (HWI).

3.3 Characteristics of heat waves across California: intensity, duration, frequency

To describe the spatial variability of heat wave characteristics, we display maps of the gridded HWI intensity, duration, and frequency by month (Fig. 4). The inland regions experience the most heat wave activity in May. This is due to the large May variance in T_{\max} anomalies (Fig. 2 bottom). At the coastal regions, the frequency of heat wave days is more evenly spread throughout the summer, with more September events, especially throughout the South Coast compared to other regions. This coastal uptick reflects the beginning of

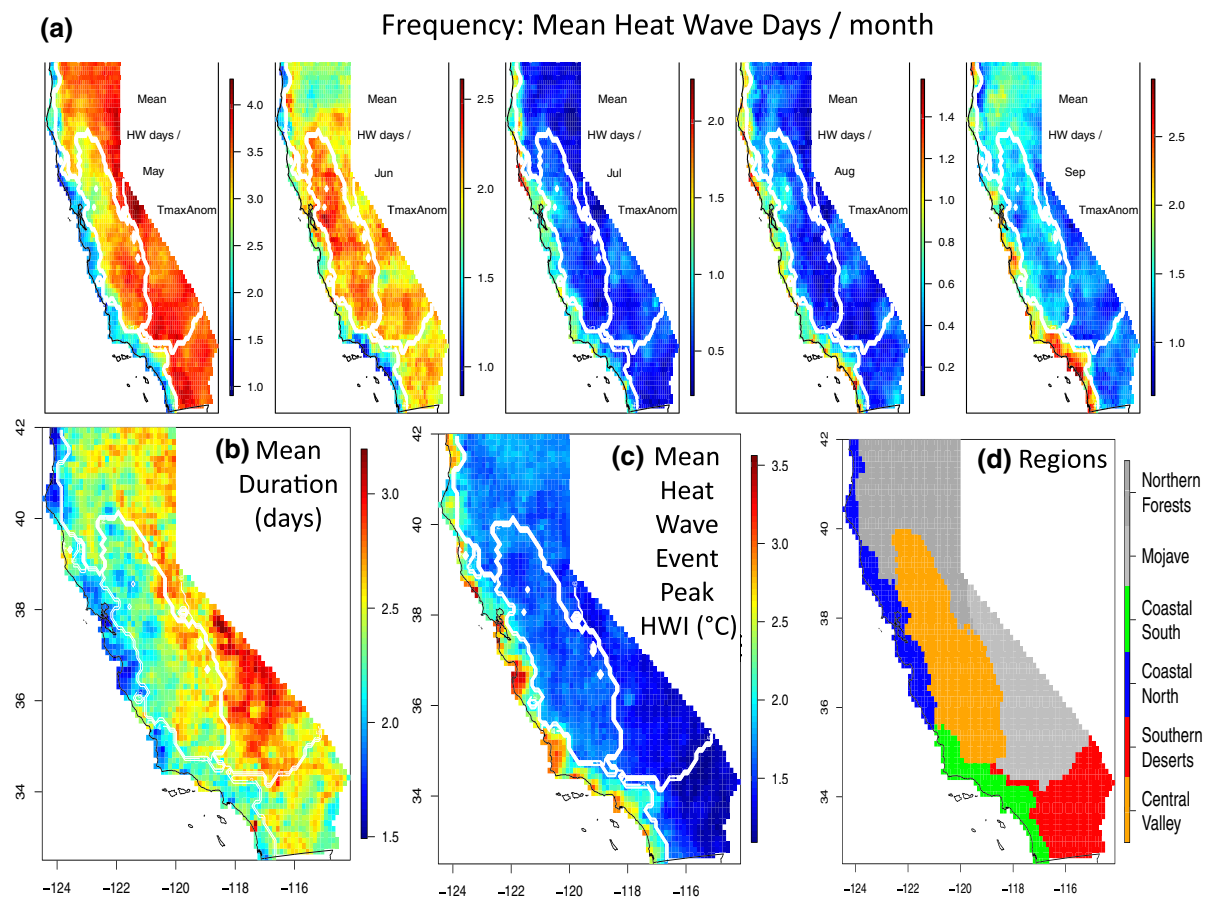


Fig. 4 Characteristic of heat waves. **a** frequency maps for each month, May through September, in average days/month (note *different color scale*). **b** Mean duration of events in days, **c** mean event peak HWI ($^{\circ}\text{C}$), **d** regions as show in Fig. 1a

the Santa Ana Wind season (Guzman Morales et al. 2016) when offshore flow episodes begin and increase into fall and winter.

Coastal heat waves tend to be shorter in duration and more intense, relative to local climate, than inland heat waves (Fig. 4 bottom). The shortest duration events, mean of ~2 days, occur along the north and south coast. The Mojave region (not discussed in detail) has the longest duration events on average. The pattern of heat wave peak intensity follows the regional coast to inland boundaries well, with mean peak intensities ~2 °C restricted to the coastal regions. While it is hotter in inland areas, heat waves at the coast are more intense in their deviation from the mild coastal climate. Other studies have noted that summertime T_{max} temperature distributions in coastal California are markedly skewed with long warm tails that indicate the potential for very intense heat waves relative to the mean climate (Guirguis et al. 2017). The spatial pattern of heat wave intensity is at least partially due to CLC. Anomalous heating of the already warm and sunny inland regions is driven largely by horizontal and vertical temperature advection. At the coast, the potential for a large change in diabatic heating (Iacobellis and Cayan 2013) adds to the advection components during extreme conditions. Heat waves defined using HWI_{raw} (not shown) show a similar spatial pattern

of duration and intensity but very different monthly frequencies as expected due to the influence of the seasonal cycle (c.f. Fig. 2). Additionally, when interpreting these heat wave statistics (Fig. 4), it is important to note the sample size. By definition, locally a heat wave day occurs at each grid cell for 5% of the record. The many small intensity and duration heat waves wash out the most intense events, which can be much longer and intense (as illustrated by the Fig. 3 case study) than the average picture depicts. In most of the following analyses we focus on the top 50 heat wave events to focus on the strongest events while achieving the same sample size between regions.

3.4 Heat waves and coastal low clouds

To investigate the propagation of heat waves through California, we composite the top 50 events for each focus region centered on the heat wave peak day (Fig. 5). Additionally, we composite the HWI at the paired region of interest and CLC of the coastal region. Through compositing two regions these time series represent the average way in which heat waves evolve in both time and space. Variability around these composites is examined in Sect. 3.5.

First we examine inland heat waves and their corresponding expression at the coast. There is a strong coastal

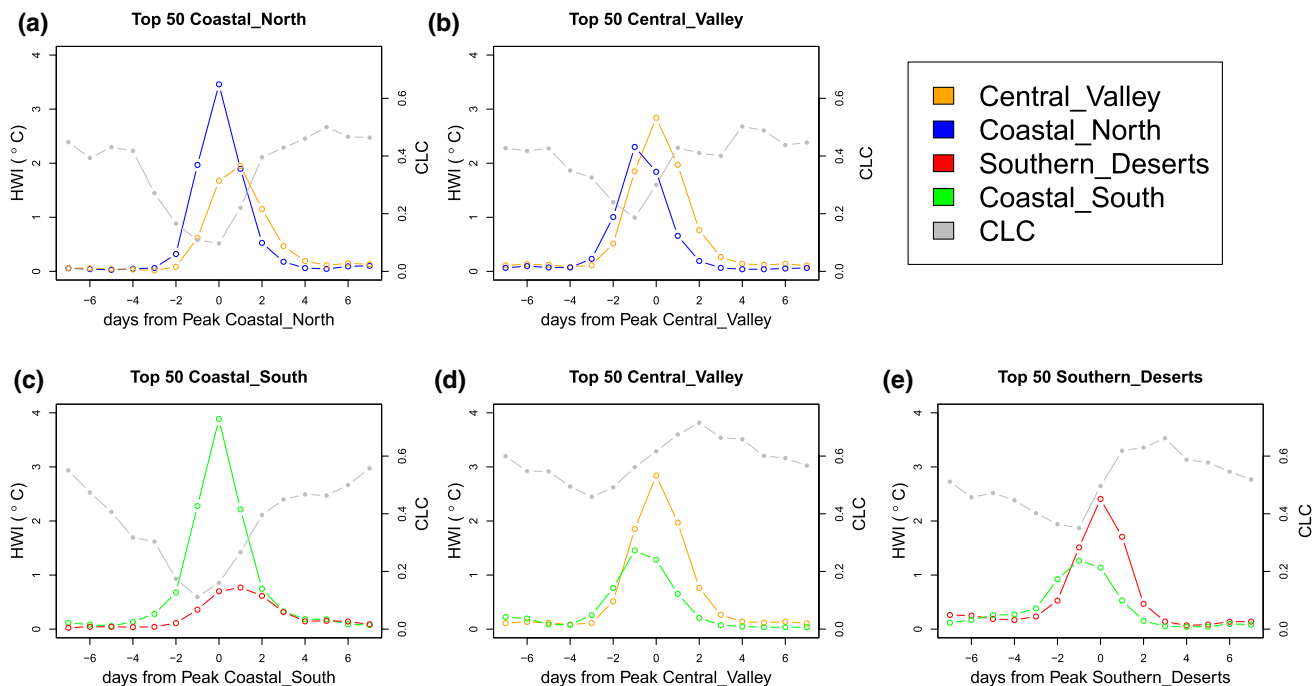


Fig. 5 HWI composites of top 50 focus region heat waves with other paired region shown and CLC for coastal region (*gray trace*). Paired regions are denoted as “focus region–paired region” **a** “Coastal North–Central Valley”, **b** “Central Valley–Coastal North”, **c** “Coastal

South–Southern Deserts”, **d** “Central Valley–Coastal South”, **e** “Southern Deserts–Coastal South”. This ordering is used for all following five *panel* figures

expression (at the North Coast) of extreme heat that peaks in intensity the day before the peak in the Central Valley (Fig. 5b). The peak in heat at the North Coast corresponds to the day with minimum low cloud cover after several days of reduced cloudiness. On the Central Valley heat wave peak day, extreme heat has already begun to lessen at the North Coast, accompanied by an increase in coastal low cloudiness over the next several days. Figure 5d compares the same Central Valley heat waves to the HWI at the South Coast, and South CLC. There is a subtle reduction in south CLC leading up to Central Valley heat waves, and then a rebound, but south CLC stays quite elevated. This reflects cases that are persistently cloudy along the South Coast during Central Valley heat waves. During Southern Desert heat waves (Fig. 5e), there is a similar coast to inland evolution as seen for the Central Valley heat waves. The South Coast heat wave expression is elevated and peaks earlier than in the Southern Deserts. While CLC decreases before the inland heat and then recovers strongly, the minimum CLC is still fairly high. The weaker South Coast peak intensity during both Southern Deserts and Central Valley heat waves reflects individual events with little to no coastal heat wave, discussed further in Sect. 3.6.

During the peak of coastal heat waves (Fig. 5a, c), there is reduced CLC as expected. Interestingly, for both north and south coast CLC tends to decrease for many days before the heat wave peak, and dramatically increases while the heat wave starts to lessen in intensity. The South Coast heat wave composites (Fig. 5c) display a large difference in the coastal heat magnitude compared to the Southern Desert magnitude. This reflects that some strong magnitude coastal heat waves occur with little or no inland extent and are likely Santa Ana wind-driven heat waves. This magnitude difference may be due, in part to the additional subsidence via mountain wave-driven subsidence/downslope warming near the coast that is absent in the deserts during Santa Ana Wind events.

Overall in these composite pictures (Fig. 5) we find that (a) regional heat waves tend to have at least some heat expression across multiple regions, although the relative intensity varies by region of interest, (b) heat waves tend to move from the coast inland, (c) CLC is dramatically reduced before and during coastal heat wave buildup and increases after the heat wave peak. This strong increase in CLC after anomalous warmth is in agreement with the case studies of Koraćin et al. (2005) and Lewis et al. (2003).

3.5 Variation in heat wave spatial intensity and timing

The composite time series (Fig. 5) depict an average picture of how heat wave events progress in time and intensity through different California regions, and the corresponding CLC. However, these composites ignore behavior of the variation around this canonical evolution. Next, we quantify

the variability in heat wave spatial intensity and temporal evolution.

We assess each heat wave event's spatial expression (Fig. 6) using the peak magnitude ratio (as described in the Sect. 2). The different region pairs show varying distributions of peak magnitude ratios. For example, during Southern Desert heat waves (Fig. 6e), the peak magnitude ratios range from 0 (no heat wave at the South Coast during a Southern Desert heat wave) to ~3 (peak heat wave intensity at the South Coast was three times the intensity of the Southern Deserts peak). Not only is the Southern Desert's peak magnitude ratio range slightly wider than the range of other regions, it also has a broader distribution across this range. The high peak magnitude ratios in the Southern Deserts may be strong coastal Santa Ana heat waves that made sufficient impact in the Southern Deserts due to strong upper level ridging to make it into the top 50 events. The South Coast's propensity towards coastally trapped heat waves with little expression in the Southern Deserts can be seen in the Fig. 6c ratio distribution which is narrower and skewed towards lower ratios. Heat waves at the North Coast (Fig. 6a) also exhibit this coastally trapped skew, although not as strongly as at the South Coast. During Central Valley heat waves, there are many cases with low intensity at the South Coast, although there is a long tail towards high ratios (Fig. 6d). Lastly, when examining the intensity of Central Valley heat waves in the North Coast (Fig. 6b), the distribution shifts closer to equal intensity between these regions (i.e. closer to ratio = 1). This tendency towards a more comparable heat wave intensity was also apparent in the similarity of Central Valley and North Coast composite peak intensities in Fig. 5b. Overall, we find more tendency for coastal heat waves to have little inland expression, particularly when comparing South Coast heat waves to their expression in the Southern Deserts. Central Valley heat waves tend to have a more shared expression with the North Coast and less with the South Coast.

To investigate the variability in the timing and direction of heat wave propagation, we compare the weighted peak timing across pairs of regions (Fig. 7). For all focus regions, the brunt of the heat wave event tends to occur at the coast before moving inland. The coastal weighted peak usually occurs about 0.5–2 days before the inland peak. While only rarely (<5%) do heat waves move from inland to the coast in the north, this directional movement happens more often (22%) for South Coast heat waves.

These Southern California inland to coast moving heat waves are related to the 4-corners upper ridge of high pressure building from east to west in June to August. This is also captured by more Southern Desert HWI_raw events (not shown), which occur in mid-summer, showing this east to west movement.

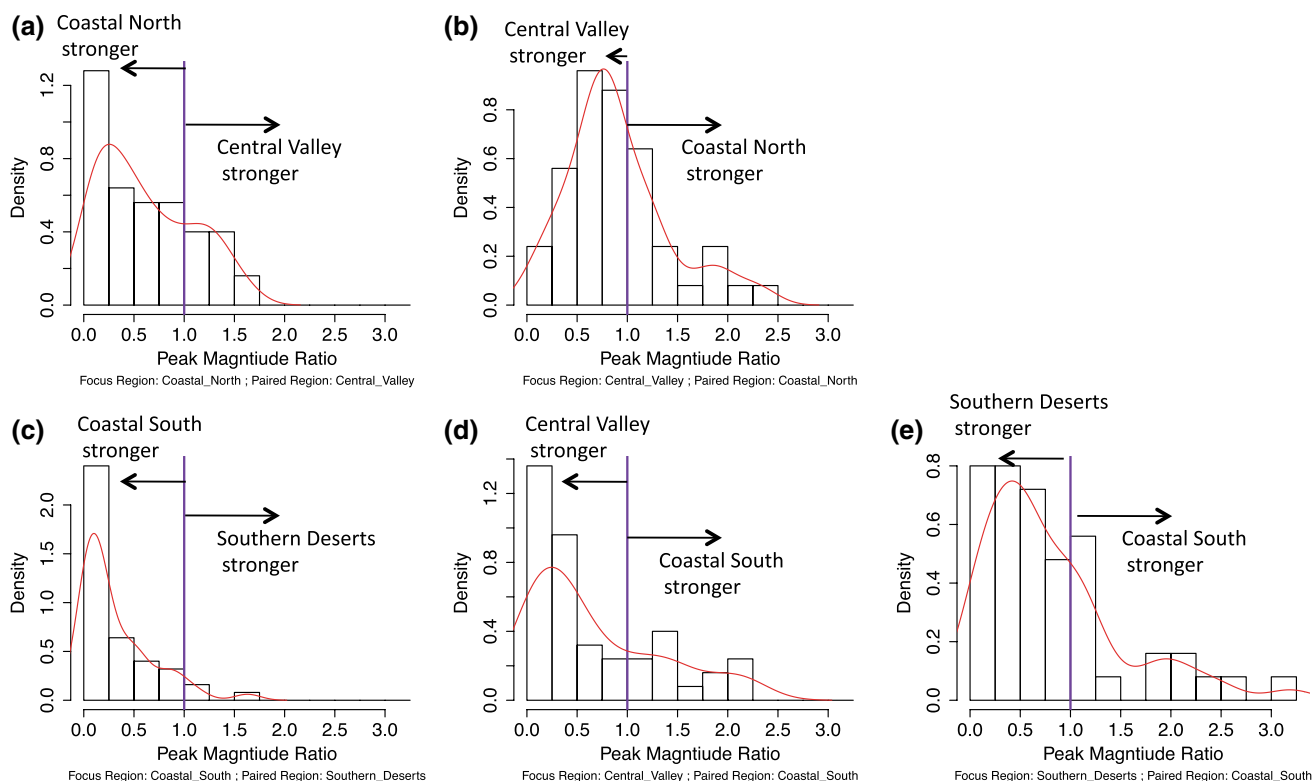


Fig. 6 Density plots of peak magnitude ratio (PMR) for top 50 heat wave of focus regions. PMR=peak HWI of paired region during focus region heat wave: peak HWI in the focus region. Purple line denotes PMR = 1, equal peak HWI in both regions. Red line denotes

Gaussian density estimation. In each panel, the focus and paired regions are provided in the text along the *x*-axis, and are the same as presented in the Fig. 5 caption

A special type of heat wave with strong coastal intensity and little inland heating (Fig. 6) includes those extreme events driven by down-slope Santa Ana winds. These katabatic winds begin to increase in frequency during September and explain the uptick in the frequency of September South Coast heat waves (Fig. 4 top). During coastal heat waves, the cooling influence of CLC is of course absent, while during inland heat waves a potential range of coastal conditions is possible. Thus, for the remainder of this paper, we will focus on the coastal expression of heat during inland heat waves. Why during some inland heat waves does the coast also experience extreme heat, while during other events the coast is buffered from extreme heat? We will examine what drives the variability in coastal heat with particular emphasis on the interplay with coastal low clouds.

3.6 Coastal low cloudiness (CLC) and coastal heat during inland heat waves

What drives the distribution in heat wave intensity at the coast during inland heat waves (Fig. 6)? To investigate the role of low clouds at the coast, we examine the top 50 inland heat waves and compare the peak coastal HWI to

CLC (Fig. 8). We find that the degree to which an inland heat wave is expressed at the coast is associated with CLC.

That is, higher intensity coastal heat events are associated with clearer conditions and when the coast is cool during an inland heat wave, enhanced CLC is present. This association is especially strong for the Central Valley–South Coast regional pair, where CLC and South Coast peak HWI are correlated at $r = -0.76$ during Central Valley heat waves. There are also moderate negative correlations for the Central Valley–North Coast pair ($r = -0.52$) and Southern Deserts–South Coast pair ($r = -0.5$). The Southern Deserts–South Coast pair exhibits more variability in CLC during weak coastal heat, while the Central Valley–South Coast pair shows the clearest signal that less coastal heat is associated with more CLC. These results (Fig. 8) suggest that CLC is an important modulating factor controlling the expression and impacts of extreme heat at the coast, especially at the South Coast during Central Valley heat waves.

Since the observations indicate that the presence of CLC during an inland heat wave can modulate the intensity of heat at the coast, next we explore what controls whether it will be cloudy or clear at the coast during inland heat waves. During all summer conditions, previous work (e.g. Clemesha

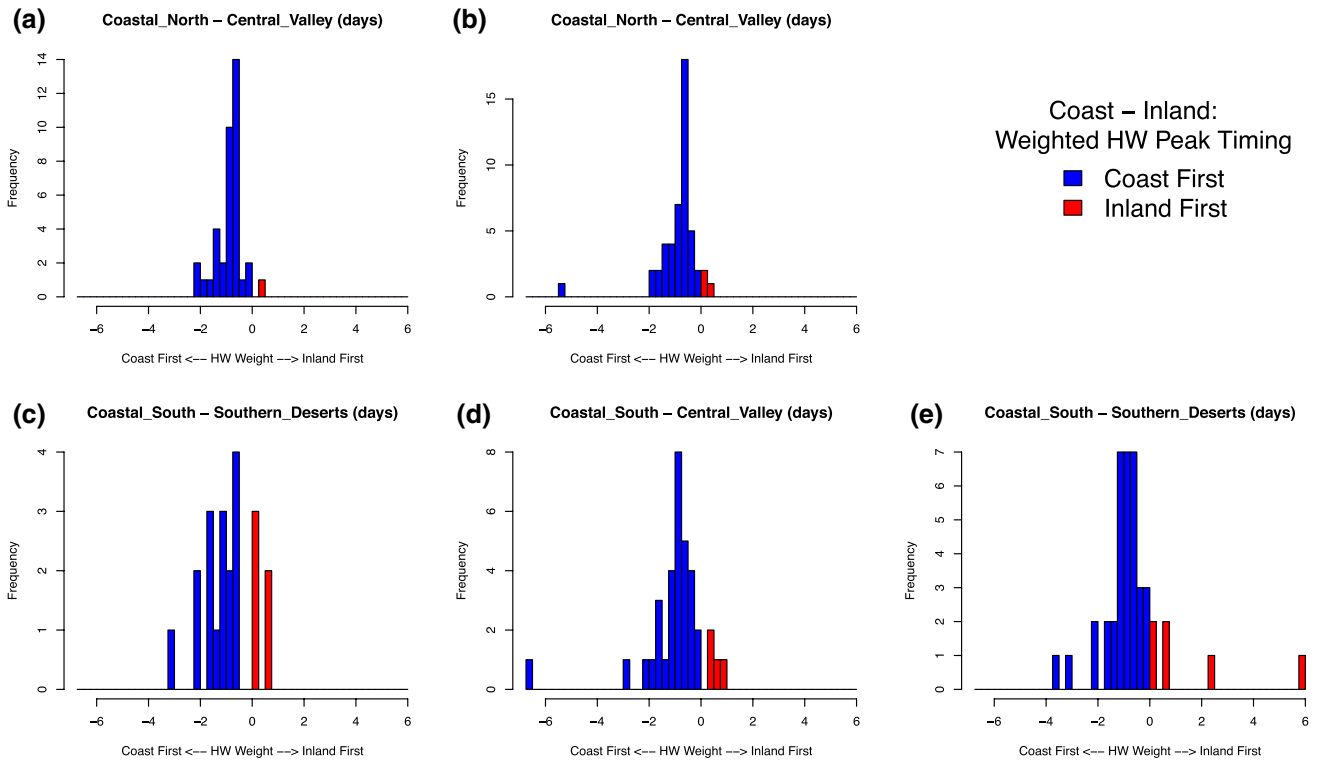


Fig. 7 Histograms of difference in weighted heat wave (HW) peak timing for focus region and paired region within ± 6 days. Differencing is always Coast Region minus Inland Region such that negative values all signify the weighted HW peak timing was at the coast first. For example, in *panel a* heat waves tend to peak at the coast up to ~ 2

days before they peak in the Central Valley (*blue bars*), while there was only one case where the peak occurred first in the Central Valley (*red bar*). Note the different sample sizes of $n=38, 48, 21, 48,$ and 41 for **a–e**, respectively, because timing is compared only for events with peak magnitude ratio >0.20

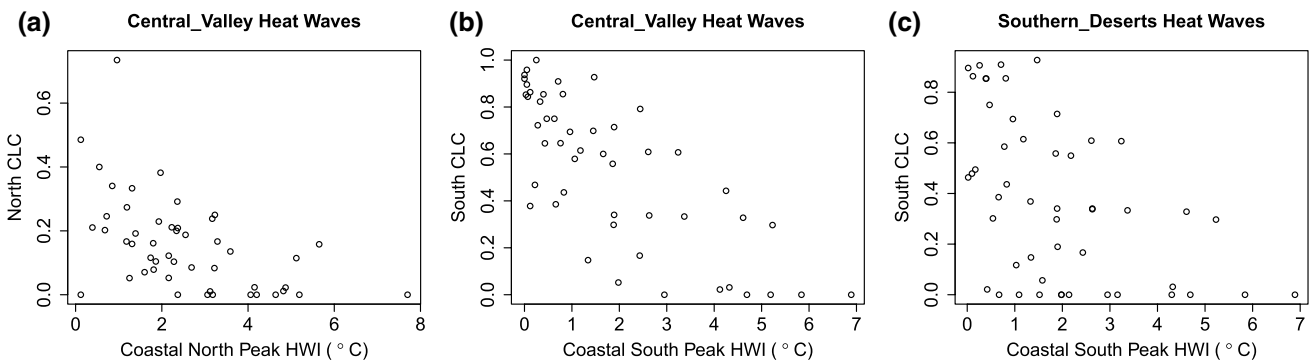


Fig. 8 Peak coastal HWI vs CLC, during top 50 inland heat waves. **a** Coastal North during Central Valley top 50 events, **b** Coastal South during Central Valley top 50 events, **c** Coastal South during Southern Deserts top 50 events. CLC on the day of the coastal HWI peak is used

et al. 2017; Iacobellis and Cayan 2013, Myers and; Norris et al. 2013) points to the importance of stability, subsidence and inversion characteristics in controlling daily CLC variability. In particular, although subsidence is a necessary condition, too much subsidence may lower the inversion base height essentially reducing the depth of or eliminating the MBL where the low clouds reside. Accordingly, CLC

and two metrics of the temperature inversion, the inversion strength (DT) and inversion base height (ZBASE), are stratified according to the following heat wave conditions. For the Central Valley–South Coast pair (Fig. 9 top) and the Southern Deserts–South Coast pair (Fig. 9 bottom), days are classified into three categories (a) “coastal and inland heat wave” ($HWI > 1\text{ }^{\circ}\text{C}$ at both regions), (b) “inland only heat

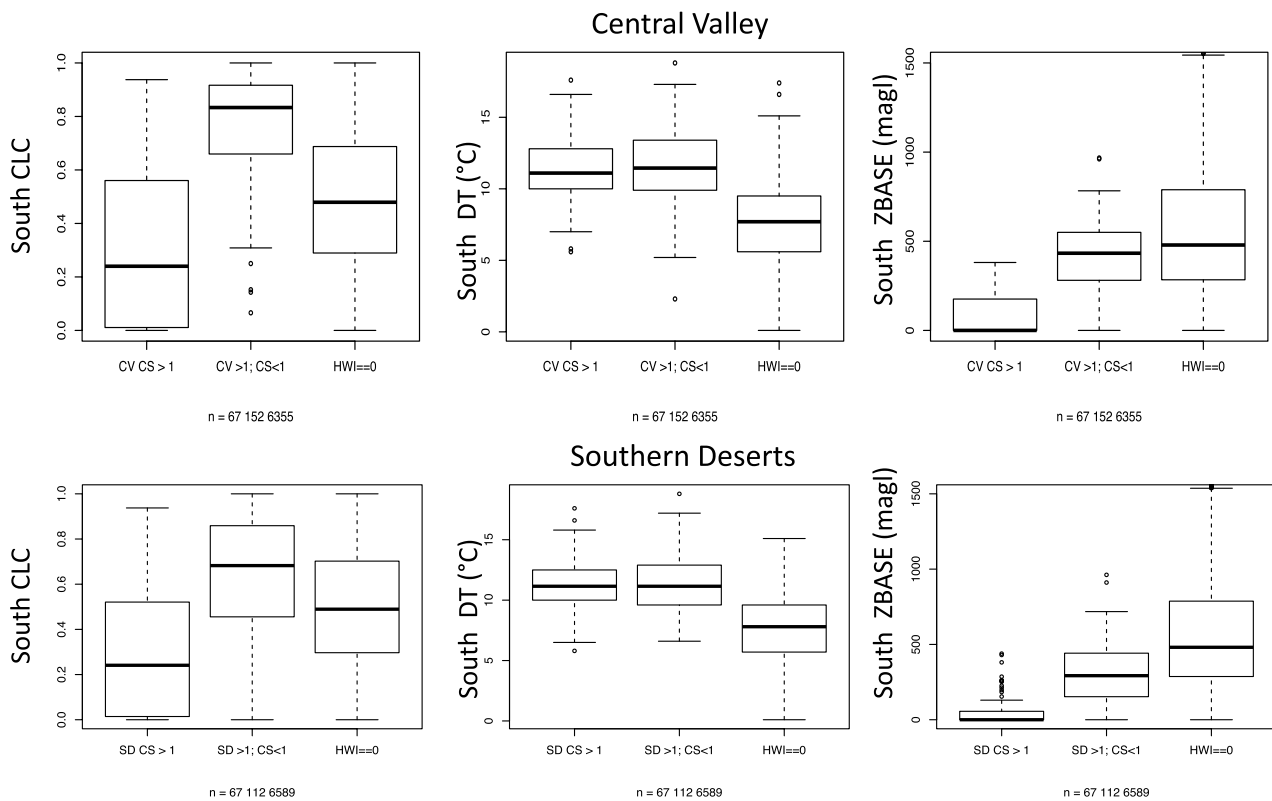


Fig. 9 Box plots during three classes, *left box* “coastal and inland heat wave” ($\text{HWI} > 1\text{ }^{\circ}\text{C}$ at both regions), *middle box* “inland only heat wave day” (inland $\text{HWI} > 1\text{ }^{\circ}\text{C}$; coastal $\text{HWI} < 1\text{ }^{\circ}\text{C}$) and *right box* “non-heat wave” ($\text{HWI} = 0\text{ }^{\circ}\text{C}$ at both regions). The coastal region is Coastal South (CS). The inland region is (top) Central Val-

ley (CV) and (bottom) Southern Deserts (SD). For (left) CLC, (middle) DT, and (right) ZBASE under 1500 meters above ground level. Median, quartiles, and 1.5 times the interquartile range denoted by *thick line*, *box*, and *whiskers*, respectively

ley (CV) and (bottom) Southern Deserts (SD). For (left) CLC, (middle) DT, and (right) ZBASE under 1500 meters above ground level. Median, quartiles, and 1.5 times the interquartile range denoted by *thick line*, *box*, and *whiskers*, respectively

wave day” (inland $\text{HWI} > 1\text{ }^{\circ}\text{C}$; coastal $\text{HWI} < 1\text{ }^{\circ}\text{C}$) and (c) “non-heat wave” ($\text{HWI} = 0\text{ }^{\circ}\text{C}$ at both regions). In agreement with Fig. 8, we find that if the coast is shielded from extreme inland heat, it is significantly more cloudy at the coast than during simultaneous coastal and inland extreme heat. Inland only Central Valley heat wave days also tend to have more South Coast CLC than normal non-heat wave days (Fig. 9 left). Inversion strengths during either heat wave class are stronger than during non-heat wave days (Fig. 9 middle). The strong inversion is a reflection of a warm upper ridge aloft during the heat wave inland. Inversions weaker than $\sim 5\text{ }^{\circ}\text{C}$ are noticeably absent for both heat wave classes, but there is no significant DT difference between the coastal and inland heat wave days versus the inland only heat wave days.

However, we find a significant difference in inversion base heights (ZBASE), contingent on presence or absence of coastal extreme heat (Fig. 9 right). Days when extreme heat is contained inland while it stays cloudier and cooler at the coast, are associated with stronger than normal inversions, but also near normal non-heat wave inversion base

heights. Days for which extreme heat reaches both the coast and inland regions, tend to have much lower inversions than the non-heat wave or inland only heat waves. These results (Fig. 9) suggest that inversion base height is more important than inversion strength in dictating if it will be cloudy or clear at the coast during inland heat waves. Furthermore, inland heat waves that have little expression at the coast tend to have coastal low cloudiness present and an inversion base height that is closer to non-heat wave conditions.

The influence of inversion base height on cloudiness and extreme heat at the coast is next scrutinized in another way by classifying days during a moderate inland heat wave (inland $\text{HWI} > 1\text{ }^{\circ}\text{C}$) by elevated ($>200\text{ m}$) and depressed ($<200\text{ m}$) South Coast ZBASE. During an inland heat wave, days with lower ZBASE tend to be associated with more intense extreme heat at the coast and less cloudiness (Fig. 10). Conversely, days with elevated ZBASE experience less extreme coastal heat and more cloudiness. While there is a clear distinction in intensity of coastal heat by these ZBASE classes, inland heat intensity does not appear

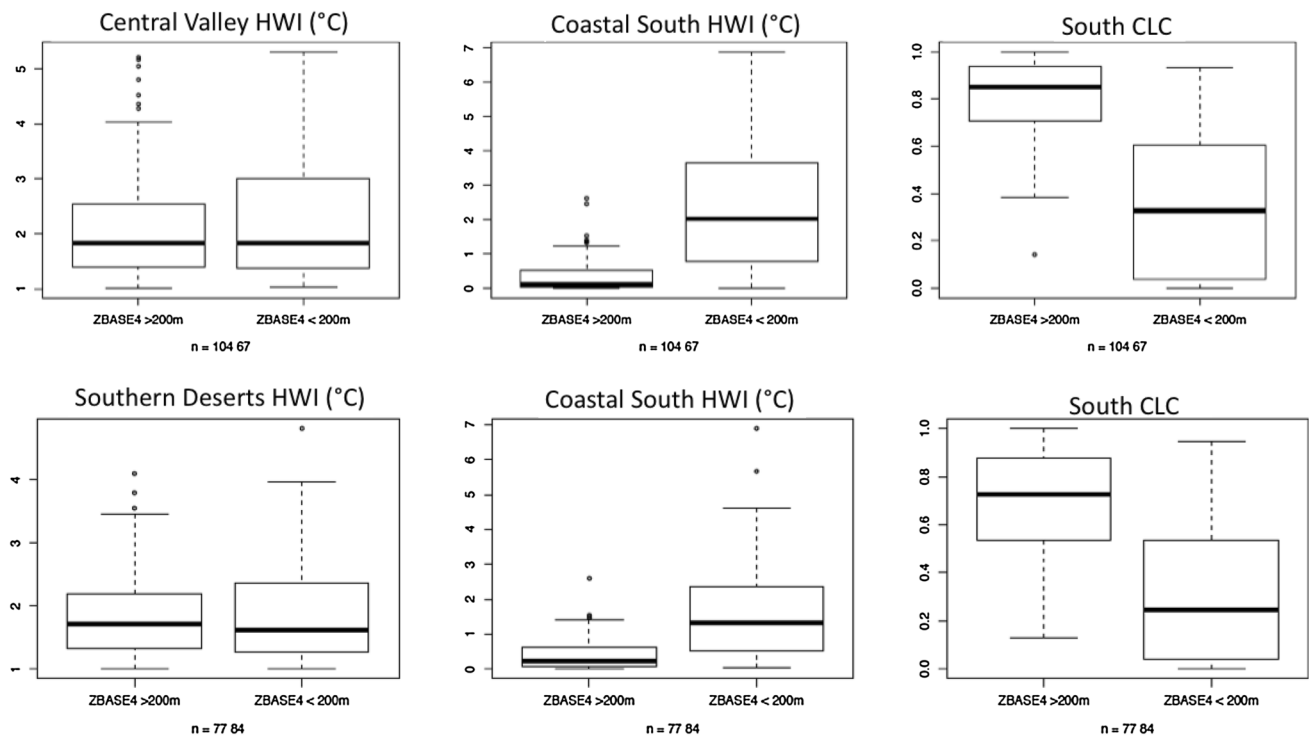


Fig. 10 Metrics during inland HWI > 1 °C at the (top) Central Valley and (bottom) Southern Deserts. Box plots during two classes left box ZBASE at four PST (ZBASE4) > 200 m and right box ZBASE4

< 200 m. For (left) HWI at inland regions, (middle) Coastal South HWI, (right) South CLC. Median, quartiles, and 1.5 times the interquartile range denoted by thick line, box, and whiskers, respectively

sensitive to these height classes (Fig. 10 left). These results suggest that accurate forecasts of inversion base height are essential in forecasting the coastal expressions of inland heat waves as they are modulated by CLC.

Motivated by the mean condition findings of Clemesha et al. (2017) that daily variability of CLC is positively related to inland surface temperatures ~ 650 – 800 km to the north, we examined the South Coast during Central Valley heat waves. As expected, of the three inland–coastal pairs examined (Fig. 8), there were more cases of very cloudy South Coast conditions during Central Valley inland heat. One such notable case is June 1960, the second highest ranking Central Valley heat wave, in which the South Coast stayed persistently very cloudy (~ 80 – 100% CLC over 9 days, Figure S2). Critically, inversion base height did not reach ground level at the South Coast (as it did in the North Coast), but stayed elevated at ~ 450 – 800 m during this time period.

3.7 Movement of heat waves through northern California

Of all California regions, the North Coast exhibits the strongest link between heat and morbidity (Guirguis et al. 2014). Central Valley heat waves typically have a near comparable HWI intensity at the North Coast (Fig. 6). Almost all of the top 50 Central Valley heat wave events examined

move from the North Coast and spread inland (Fig. 7). To further elucidate the drivers of these temporal and spatial attributes of major northern California heat waves, we composite HWI, near surface winds, and anomalies of Z500, SLP, and ω_{850} . These composites (Figs. 11, 12) are created using the top 5 Central Valley heat waves which are centered on these peak dates (from rank 1 to 5): 06/15/61, 06/03/60, 05/07/87, 05/13/76, 05/17/08.

From Fig. 11, a significant upper level trough and corresponding surface low pressure develop barotropically in the Gulf of Alaska about 5 days before major heat waves peak in the Central Valley. Then on day -3 a significant upper ridge and surface high pressure set-up along the Pacific Northwest coast and intensify. Seaward and adjacent to the high pressure over the western continent a surface low becomes significant in strength by day -1 . Anomalous subsidence over the region starts on day -4 , is strongest on day -2 , and most widespread on day -1 . From Fig. 12, surface winds are strongly northwesterly along the California coast and westerly over the mid Central Valley region on day -5 . In accordance with the changing surface pressure pattern, the winds in the Central Valley and landward shift to offshore. On day -1 (1 day before the Central Valley peak), the heat wave intensity is at its maximum at the North Coast, and the surface flow over land is northeasterly (and easterly at the north end of the Central Valley). As the offshore flow

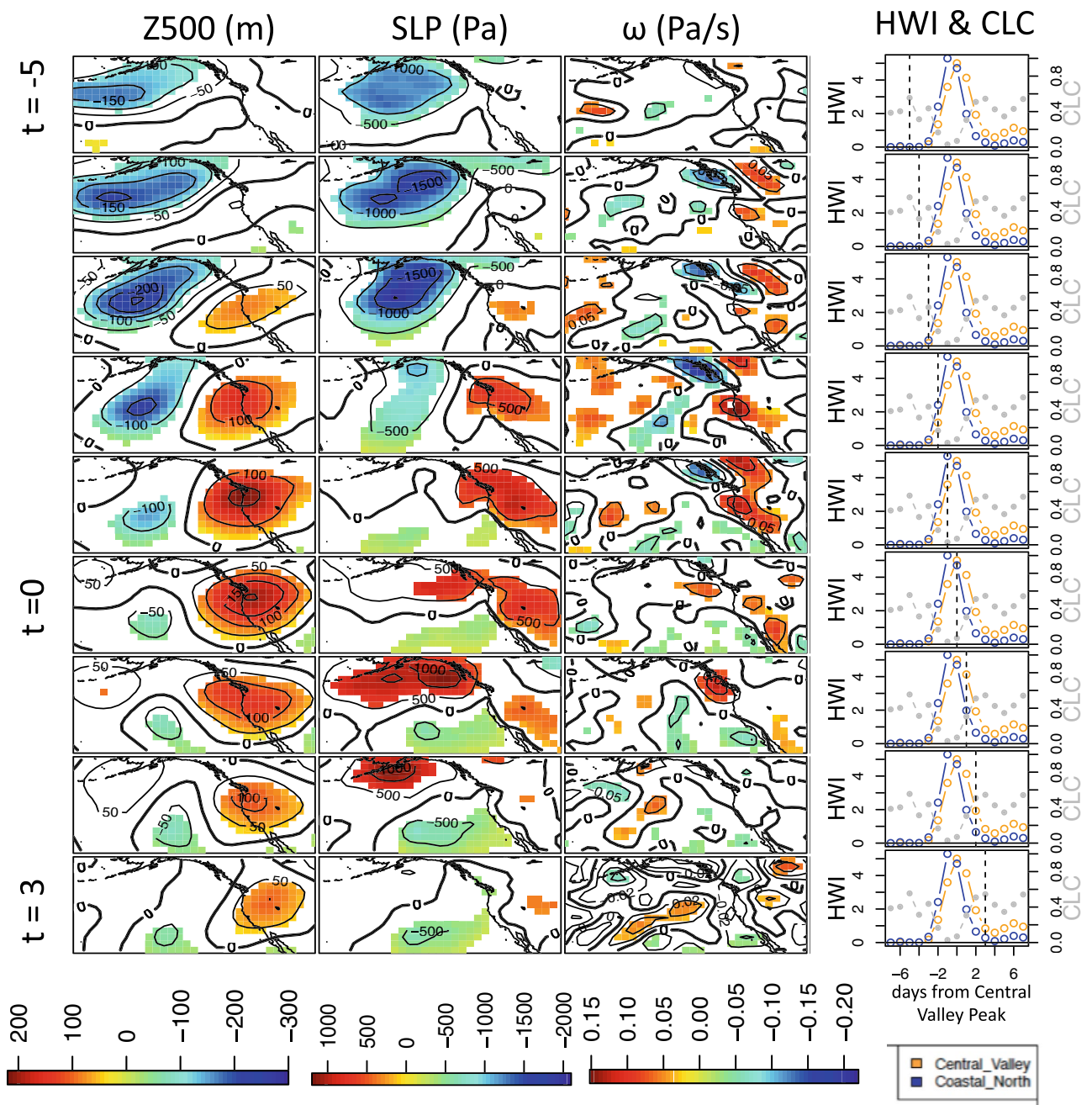


Fig. 11 Composite during the five greatest Central Valley heat waves. From $t = -5$ to $t + 3$, where $t = 0$ is the Central Valley peak HWI. Z500, SLP, ω anomalies. Only values statistically significant with 95% confidence (two-tailed test) determined via bootstrap resampling (performed with 500 resampled 5-date composite anomaly maps) are

plotted in color. (Right) Composite times series of Central Valley HWI (orange) and Coastal North HWI (blue), and north CLC (gray), dashed black line denotes day of maps. See Fig. 12 for associated HWI maps

weakens on day = 0, extreme heat moves inland from the North Coast to the Central Valley. After the peak of the heat wave, winds return to onshore flow, CLC starts to increase at the coast, and the extreme heat lessens first at the North Coast before lessening in the Central Valley. The surface high pressure weakens before the upper level ridge fully

diminishes. The resulting typical pattern is that heat wave events peak in intensity about a day earlier at the North Coast than in the Central Valley.

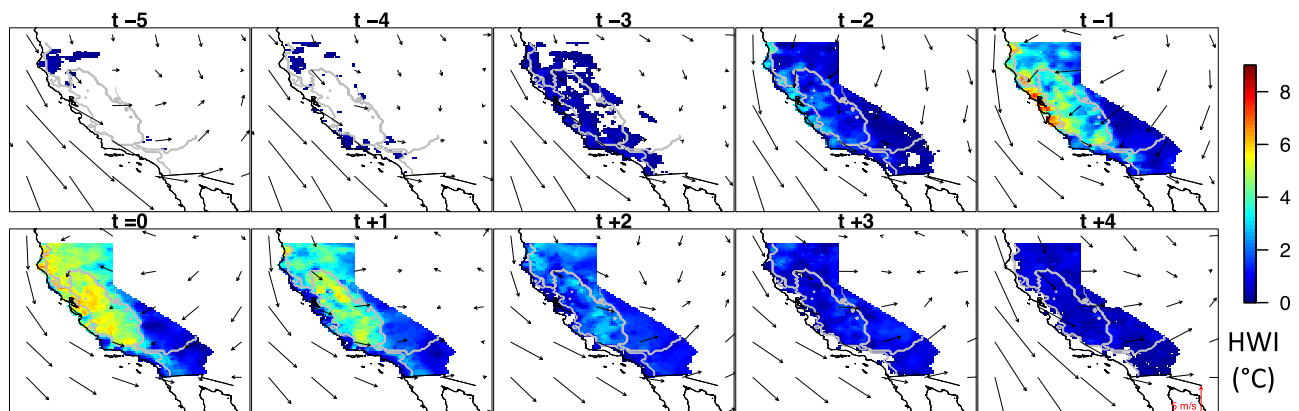


Fig. 12 As in Fig. 11, composite during the five greatest Central Valley heat waves, showing gridded HWI and near surface winds overlain. From $t-5$ to $t+4$

4 Summary and conclusions

In this paper, we assess California heat wave spatial and temporal expression at the coast and inland, while considering one of the key modulating factors of summertime coastal climate—coastal low cloudiness (CLC). While previously more attention has been given to the absolute hottest days and/or nights (e.g. Gershunov et al. 2009; Gershunov and Guirguis 2012; Grotjahn and Faure 2008), here we focus on the unseasonably warm events which often cluster in the shoulder seasons (Figs. 2, 4), and may also result in significant human health impacts. Early-season events in particular are known to be harmful to health since the population has not had time to adequately acclimate to hot weather (e.g. Basu and Samet 2002; Ebi et al. 2004; Guirguis et al. 2014).

Observations indicate that characteristics of extreme heat events are variable throughout California. Heat wave events tend to be shorter, but more anomalously intense along the coast. These features of coastal heat waves may have competing effects on the health of coastal residents. Furthermore, this work examined the spatial and temporal movement of individual heat wave events. This event-centered framework uncovered features of California heat waves, such as their inland progression, that would be lost if examined in an aggregate method. That is, for heat wave events with a strong impact across regions, the coast typically feels the initial effects first, as well as the end of the extreme weather before inland areas (Figs. 5, 7). Thus, the timing of inland heat impacts can be gauged by monitoring the eastward progression of heat waves and the shifting axis of the upper ridge. Conversely, forecasting the beginning of coastal heat waves is a greater operational challenge since the impacts are felt at the coast first. Furthermore, accurate forecasts of inversion base heights, which we have shown (Figs. 9, 10)

are critical to the coastal expression of heat waves as they are modulated by CLC, are needed.

Our analyses also uncover the progression and variability of coastal low cloudiness during heat wave events. The beginning of coastal heat waves are associated with a loss of CLC, followed by a strong rebound of CLC starting close to the peak in heat wave intensity. While it is clear at the coast during coastal heat wave onset, this paper identified some important factors influencing heat and cloudiness at the coast during cases of inland heat waves. The degree to which an inland heat wave is expressed at the coast is associated with the presence of low clouds. This suggests that CLC is an important modulating factor controlling the expression and impacts of extreme heat at the coast. This relationship is especially true for the South Coast during Central Valley heat waves. In agreement, with the findings of Clemesha et al. (2017) that daily CLC variability is positively related to T_{\max} ~650–800 km to the north, there are cases when the South Coast stays persistently cloudy and protected from extreme heat while a heat wave impacts the Central Valley.

We demonstrate that during inland heat waves, the height of the inversion base (ZBASE), which caps the marine boundary layer, is a key factor determining coastal cloudiness, and thus, coastal heat expressions. During inland heat waves the coastal inversion strength (DT), tends to be stronger than during average non-heat wave conditions, but DT has less influence on CLC during inland heat waves than ZBASE. This is in agreement with the findings of Iacobellis and Cayan (2013), that CLC over land is more related to ZBASE, and CLC over the coastal waters is more related to DT. The importance of ZBASE in forecasting CLC over land has also been recognized by solar resource researchers (Zhong et al. 2017). Since there are past cases when the inversion is strong but elevated and maintenance of coastal cloudiness buffers the coast from extreme heat, long term

trends in inversion characteristics may cause changes to CLC and thus, coastal heat waves. Using the same California radi-sonde sites as used here, Iacobellis et al. (2010) reported an increase in ZBASE and a decrease in DT from 1960 to 2007. Although they also found using GCMs that inversion strength is projected to grow over the twenty-first century, and that from the mid 1970s–2007 inversion strength has increased in the observational record. Many others also report a projected increase in metrics related to inversion strength (Williams et al. 2015; Myers and Norris 2016; Qu et al. 2014). Although determining the future of ZBASE is more challenging, our results and those of Iacobellis and Cayan (2013) suggest that inversion height is more critical than strength in determining CLC for the coastal terrestrial swath, where large populations reside. An urbanization driven trend towards higher cloud base height is also at play in southern California (Williams et al. 2015). Future changes in CLC will have impacts on mean climate and may also change the coastal expression of extreme heat events.

We also show that heat wave events typically impact both coastal and inland regions, although there is greater propensity towards coastally trapped events rather than inland confined events. A future investigation of summer and fall coastally trapped heat waves will involve a higher resolution investigation of winds including hot offshore Santa Ana winds, cool sea breezes, and eddy circulations. This work described the evolution and variability of coastal and inland heat waves in the observational record, paving the way to more accurately assessing impacts of future California heat waves in forecasts and downscaled model projections.

Acknowledgements We are thankful for support from NOAA Coastal and Ocean Climate Applications (COCA) program grant NA15OAR4310114. This study supports the climate science education efforts of Climate Education Partners, a project funded by a National Science Foundation Grant #DUE-1239797. The study also contributes to DOI's Southwest Climate Science Center activities and to NOAA's California and Nevada Applications Program. NCEP Reanalysis data are provided by the NOAA/OAR/ESRL PSD, Boulder, Colorado, USA, from their website at esrl.noaa.gov/psd. Radiosonde Database at esrl.noaa.gov/raobs/.

References

- Basu R, Samet JM (2002) Relation between elevated ambient temperature and mortality: A review of the epidemiological evidence. *Epidemiol Rev* 24:190–202
- Clemesha RES, Gershunov A, Iacobellis SF, Williams AP, Cayan DR (2016) The northward march of summer low cloudiness along the California coast. *Geophys Res Lett*. doi:10.1002/2015GL067081
- Clemesha RES, Gershunov A, Iacobellis SF, Cayan DR (2017) Daily variability of California coastal low cloudiness: a balancing act between stability and subsidence. *Geophys Res Lett*. doi:10.1002/2017GL073075
- Ebi KL, Teisberg TJ, Kalkstein LS, Robinson L, Weiher RF (2004) Heat watch/warning systems save lives: estimated costs and benefits for Philadelphia 1995–98. *Bull Am Meteor Soc* 85:1067–1073
- Gershunov A, Guirguis K (2012) California heat waves in the present and future. *Geophys Res Lett* 39:L18710. doi:10.1029/2012GL052979
- Gershunov A, Cayan D, Iacobellis S (2009) The great 2006 heat wave over California and Nevada: signal of an increasing trend. *J Clim* 22:6181–6203. doi:10.1175/2009JCLI2465.1
- Grotjahn R, Faure G (2008) Composite predictor maps of extraordinary weather events in the Sacramento, California, region. *Weather Forecast* 23(3):313–335
- Grotjahn R, Black R, Leung R, Wehner MF, Barlow M, Bosilovich M, Lee YY (2016) North American extreme temperature events and related large scale meteorological patterns: a review of statistical methods, dynamics, modeling, and trends. *Clim Dyn* 46(3–4):1151–1184
- Guirguis K, Gershunov A, Tardy A, Basu R (2014) The impact of recent heat waves on human health in California. *J Appl Meteorol Climatol* 53(1):3–19. doi:10.1175/JAMC-D-13-0130.1
- Guirguis K, Gershunov A, Cayan DR, Pierce DW (2017) Heat wave probability in the changing climate of the Southwest US. *Clim Dyn*. doi:10.1007/s00382-017-3850-3 (in press)
- Guzman-Morales J, Gershunov A, Theiss J, Li H, Cayan D (2016) Santa Ana Winds of Southern California: Their climatology, extremes, and behavior spanning six and a half decades. *Geophys Res Lett* 43:2827–2834. doi:10.1002/2016GL067887
- Iacobellis SF, Cayan DR (2013) The variability of California summertime marine stratus: impacts on surface air temperatures. *J Geophys Res Atmos* 118:9105–9122. doi:10.1002/jgrd.50652
- Iacobellis SF, Cayan DR, Norris JR, Kanamitsu M (2010) Impact of climate change on the frequency and intensity of low-level temperature inversions in California. Final Report to the California Air Resources Board Project 06-319. <http://www.arb.ca.gov/research/apr/past/06-319.pdf>
- Kalnay E et al (1996) The NCEP/NCAR 40-year reanalysis project. *Bull Am Meteorol Soc* 77(3):437–471
- Klein SA, Hartmann DL, Norris JR (1995) On the relationships among low-cloud structure, sea surface temperature, and atmospheric circulation in the summertime northeast Pacific. *J Clim* 8(5):1140–1155. doi:10.1175/1520-0442
- Knowlton K, Rotkin-Ellman M, King G, Margolis HG, Smith D, Solomon G, Trent, English P (2009) The 2006 California heat wave: impacts on hospitalizations and emergency department visits. *Env Health Persp* 117:61–67
- Koračin D, Leipper DF, Lewis JM (2005) Modeling sea fog on the US California coast during a hot spell event. *Geofizika* 22(1):59–82
- Leipper DF (1994) Fog on the United States West Coast: a review. *Bull Am Meteorol Soc* 75:229–240
- Lewis J, Koračin D, Rabin R, Businger J (2003). Sea fog off the California coast: Viewed in the context of transient weather systems. *J Geophys Res Atmos* 108(D15)
- Maurer EP, Wood AW, Adam JC, Lettenmaier DP, Nijssen B (2002) A long-term hydrologically-based data set of land surface fluxes and states for the conterminous United States. *J Clim* 15:3237–3251. doi:10.1175/1520-0442(2002)015<3237:ALTHBD>2.0.CO;2
- Myers TA, Norris JR (2013) Observational evidence that enhanced subsidence reduces subtropical marine boundary layer cloudiness. *J Clim* 26(19):7507–7524
- National Weather Service (2012) Heat: a major killer. (<http://www.nws.noaa.gov/os/heat/index.shtml>)
- O'Brien TA (2011) The recent past and possible future decline of California coastal fog, Doctoral thesis, p 193, Univ. of Calif., Santa Cruz, Calif
- O'Brien TA, Sloan LC, Chuang PY, Faloona IC, Johnstone JA (2012). Multidecadal simulation of coastal fog with a regional climate model. *Clim Dyn* 1–12

- Ostro BD, Roth LA, Green RS, Basu R (2009) Estimating the mortality effect of the July 2006 California heat wave. *Environ Res* 109:614–619
- Qu X, Hall A, Klein SA, Caldwell PM (2014) On the spread of changes in marine low cloud cover in climate model simulations of the 21st century. *Clim Dyn* 42(9–10):2603–2626. doi:[10.1007/s00382-013-1945-z](https://doi.org/10.1007/s00382-013-1945-z)
- Schwartz RE, Gershunov A, Iacobellis SF, Cayan DR (2014) North American west coast summer low cloudiness: broadscale variability associated with sea surface temperature. *Geophys Res Lett* 41:3307–3314. doi:[10.1002/2014GL059825](https://doi.org/10.1002/2014GL059825)
- Small I (2006) Forecasters handbook for extreme southwest california based on short term climatological approximations Part 1—The marine layer and its effects on precipitation and heating, NOAA Technical Memorandum NWS WR-277
- Williams AP, Schwartz RE, Iacobellis S, Seager R, Cook BI, Still CJ, Husak G, Michaelsen J (2015) Urbanization causes increased cloud base height and decreased fog in coastal Southern California. *Geophys Res Lett*. 42. doi:[10.1002/2015GL063266](https://doi.org/10.1002/2015GL063266)
- Zhong X, Sahu DK, Kleissl J (2017) WRF inversion base height ensembles for simulating marine boundary layer stratocumulus. *Sol Energy* 146:50–64. doi:[10.1016/j.solener.2017.02.021](https://doi.org/10.1016/j.solener.2017.02.021)